energies

Article

Investigation of Heat Transfer Fluids Using a Solar Concentrator for Medium Temperature Storage Receiver Systems and Applications

Pawan Kumar Kuldeep [1], Sandeep Kumar [1], Mohammed Saquib Khan [2], Hitesh Panchal [3], Ashmore Mawire [4] and Sunita Mahavar [1,*]

[1] Department of Physics, University of Rajasthan, Jaipur 302015, India
[2] Materials Research Centre, MNIT, Jaipur 302017, India
[3] Mechanical Engineering Department, Government Engineering College, Patan 384265, India
[4] Department of Physics and Electronics, Material Science, Innovation and Modelling (MaSIM) Research Focus Area, North-West University (Mafikeng Campus), Private Bag X2046, Mmabatho 2735, South Africa
* Correspondence: smjpr1986@gmail.com

Citation: Kuldeep, P.K.; Kumar, S.; Khan, M.S.; Panchal, H.; Mawire, A.; Mahavar, S. Investigation of Heat Transfer Fluids Using a Solar Concentrator for Medium Temperature Storage Receiver Systems and Applications. *Energies* **2022**, *15*, 7868. https://doi.org/10.3390/en15217868

Academic Editor: Carlo Renno

Received: 28 September 2022
Accepted: 21 October 2022
Published: 24 October 2022

Abstract: Solar concentrator collectors have the potential of meeting the medium- and high-temperature thermal energy demands of the world. A heat transfer fluid (HTF) is a vital component of a concentrating system to transfer and store thermal energy. This paper presents the design development of a solar paraboloidal dish concentrator (SPDC) and a study of selected HTFs using the storage receiver system of the concentrator. The locally designed SPDC (diameter 1.21 m and height 0.20 m) has features like light weight, effortless tracking, convenient transportation along with high optical and thermal performance. Three HTFs, silicone oil (SO), engine oil (EO) and ethylene glycol (EG), are selected based on their favorable properties for medium temperature (150–300 °C) applications. The characteristic parameters of HTFs, heating rate (R_h), instant thermal efficiency (η_{ith}) and the overall heat loss coefficient (U_L), are illustrated and determined experimentally. A new characteristic parameter, the normalized maximum fluid temperature (T_{nf}), is also introduced in the paper. In the heating test, the maximum attained temperatures by fluids, SO, EO and EG are found to be 240 °C, 180 °C and 160 °C, respectively. The thermal efficiencies of SO, EO and EG are determined to be 45, 36 and 31%, respectively. The heating rate of 6.56 °C/s is found to be the maximum for SO. Through the cooling test, the overall heat loss coefficient (U_L) is computed to be 14 W/mK, which is the least among the three fluids compared. The high thermal performance, environmental safety and chemical stability of silicone oil make it suitable for use in concentrators for medium-temperature heat transfer and storage applications.

Keywords: heat transfer fluids; receiver storage system; silicone oil; ethylene glycol; engine oil; solar concentrator

1. Introduction

Solar energy can be harnessed by non-concentrating or concentrating solar thermal collectors (STC). Five main solar concentrator technologies can be identified as (i) Compound Parabolic Concentrator, (ii) Parabolic Trough Concentrator, (iii) Linear Fresnel Reflector, (iv) Parabolic dish with fixed focus, (v) and a Parabolic dish with a moving focus [1–4]. In solar concentrators, the generated heat is collected, transported and stored through a heat transfer fluid (HTF) for low to high temperature applications. The heat collection is governed by the optical and thermal parameters of a concentrator system and the properties of the selected HTF. The selection of an appropriate HTF is vital to minimize the cost of the concentrator receiver, heat exchanger and heat storage with high cyclic efficiency [2]. Water is the most common low-temperature HTF, but for medium/high temperature use, it has to undergo a phase change. A number of researchers have investigated various types of sensible HTFs for solar concentrators based on their applications (medium 100–300 °C to high temperature 300–800 °C), thermochemical properties and economic feasibility. The solar concentrator HTFs can be broadly categorized as (i) Thermal oil (Therminol VP-1, Dowtherm, Mobiltherm, Mineral oil etc.), (ii) Molten salts (HITEC, HITEC XL, solar salt, etc.), and (iii) Liquid metals (Lead-Bismuth, Liquid sodium, Eutectic etc.) and other as nanoparticle suspensions in different base HTFs (nanofluids) [5,6]. A detailed review of the HTFs for use in solar power plant is presented by Benoit et al. [5]. Different thermophysical properties and heat transfer correlations for receivers are presented in this review. The review presented by Vignarooban et al. [6] includes the current status (thermal properties and stability) of various HTFs, namely, molten salts, steam, organic fluids, thermal oils, liquid metals and air. Malviya et al. [7] conducted a review on various HTFs (sodium salt, HITEC-XL, solar salt, solar grade oil, etc.) for use in parabolic trough collector. A theoretical study of various HTFs (Therminol VP-1, Syltherm 800, Solar salt, Hitec XL and liquid sodium etc.) has also been conducted by Zaharil and Hasanuzzaman [8] for Malaysian conditions. Conroy et al. [9] have developed a theoretical model to investigate hydraulic flow properties of liquid sodium, molten salt and lead-bismuth in a CSP receiver. Trabelsi et al. [10] carried out an optimization study (namely, field size, storage system and HTFs) of a solar parabolic trough power plant through the simulation software, SAM, and concluded that molten salt is economically reasonable than the synthetic oil and Therminol VPI. An evaluation of the thermal and physical properties of liquid sodium and Hitec (that is, a mixture of KNO_3, $NaNO_2$ and $NaNO_3$) was carried out by Boerema et al. [2]. It is found that liquid sodium is a suitable substitute for molten salts in future CSP. Kenda et al. [11] have studied Jatropha crude oil as an alternative HTF or thermal energy storage material (TES) and found that this oil is appropriate for a small CSP plant working near a temperature of 210 °C. Hoffmann et al. [12] have studied and compared different vegetable oils, namely, sunflower, soybean, jatropha, etc. in the medium temperature range for innovative HTFs/TES in CSP. The theoretical and experimental work carried out on different solar thermal systems with various sensible HTFs are summarized in Table 1. The table does not include work on nanofluids as it is not related to the present work.

Table 1. Review on different HTFs and their solar application.

Reference	Fluid	Solar Appliance	Application	Temperature (°C)
Boerema et al. [2]	Hitec and Liquid sodium (Na)	CSP	HTF	585/873
Trabelsi et al. [10]	Therminol VPI and Molten Salt	CSP	TES	400/593
Kenda et al. [11]	Jatropha curcas crude oil	CSP	HTF/TES	210
Hoffman et al. [12]	Seven vegetable oils	CSP	HTF	upto 250
Nkwetta et al. [13]	Dow-corning 550 silicon oil	ETC (non-concentrating)	HTF	67
Jung et al. [14]	Silicone fluid (HELISOL® 5)	CSP	HTF	450
Peng et al. [15]	Molten salt	Property study		550
Qoaidera et al. [16]	Mobiltherm 603	CSP	HTF	300
Perez-Tavernier et al. [17]	Propylene glycol:water mixture (30:70% mass ratio)	ETC (non-concentrating)	HTF	Low temp. 50
Jadhav and Venkatraj [18]	Liquid Sodium, Hitec XL and Steam	CSP	HTF	600, 873

Table 1 reveals that only a few references have quoted silicone oil (SO) as heat transfer fluids. An experimental investigation of Dow-corning 550 silicon oil was performed by Vignarooban et al. [6]. Good thermal characteristics, low corrosivity and flammability are some important reported features of this oil [6]. Nkwetta et al. [13] have also examined the thermal performance of Dow-corning 550 silicon oil for one non-concentrating and two concentrating evacuated tube heat pipes. Improved efficiency and high energy collection in comparison to pressurized water were reported in the paper [13]. High temperature stability of a HTF, HELISOL® from Wacker Chemie AG, which was a silicone-based HTF, was explored by Jung et al. [14]. The overheating (1000 h at 465 °C) of this fluid did not produce any coke-like product due to the PDMS (polydimethylsiloxane) base, while a degradation of DPO (diphenyl oxide)/BP (biphenyl) based fluids (namely, Therminol VP-1, Dowtherm A) was observed in the study [14]. Based on these reported studies in favor of SO as a suitable HTF for high temperature range, the present work is focused on an experimental investigation of SO using a small solar paraboloidal concentrator. The other synthetic oils, diesel engine oil and ethylene glycol (rarely tested), are also considered in the present study. The studies on small-size solar paraboloidal concentrators (diameter 1 to 2 m) are briefly presented in Table 2. This table shows that using storage receiver systems either stagnation test (empty receiver) or sensible heating test with water as the HTF is performed for testing of the concentrators. Tables 1 and 2 illustrate that only a few references [6,13,14] have investigated different thermal properties of silicone oil, and testing was conducted on evacuated tube solar collectors (ETC). According to the reviewed literature, no study has been conducted to test the performance of SO using a paraboloidal concentrator. The other two selected synthetic oils have also not been studied. Therefore, in the present work, an experimental study is focused on these materials to find a moderate approach for practical use of these materials in medium temperature (150–300 °C) heat transfer and storage applications. The paper includes the design details, and fabrication of a solar paraboloidal dish concentrator (SPDC) based on optical performance parameters. A comparative experimental study of the selected synthetic oils is conducted on a number of days. The characteristic parameters, namely, instant thermal efficiency η_{ith} of the concentrator with different HTFs, heating rates (R_h) and overall heat loss coefficients (U_L) of HTFs, are determined through thermal performance. A new characteristic parameter, normalized maximum fluid temperature (T_{nf}), is introduced in the paper. The introduced parameters are computed and based on the experimental observation, and recommendations are made for the selected HTFs.

Table 2. Design parameters of small size solar concentrator.

Ref.	Dish Dimensions			Receiver Details				Thermal Parameters	
	Dia. (m)	**Focal (m)**	**Height (m)**	**Material**	**Shape**	**Dia. (m)**	**Fluid**	**Efficiency (%)**	**Max. Temp. (°C)**
Ouederni et al. [19]	2.2	0.75	0.4	SS & copper	Dish	0.12	No	27	375
Mohammed [20]	1.67	0.58	0.30	Aluminium	Cylinderical	0.14	Water	50	100
Omara and Eltawil [21]	1.0	0.40	0.20	-	-	-	Brackish water	34	101
Subramani et al. [22]	1.5	0.74	0.19	Copper	Conical cavity	0.008	Water	77	97
Hassan et al. [23]	1.0	1.02	-	Copper	Cylindr-ical & Conical	0.17	Water	59–62	80
Mahavar et al. [24]	1.21	0.45	0.20	Copper	Cylindr-ical		Water with charcoal	-	80
Kumar & Yadav [25]	1.83	0.784	-	Anodized Aluminium	Sheet	0.15	No		309

2. Methodology

2.1. Performance Parameters of Solar Concentrator

The basic elements of a solar paraboloidal dish concentrator (SPDC) system are: (i) the reflector (ii), receiver (iii), tracking system and (iv) a storage system. The incident sunlight reflects through the reflector surface and concentrates at a receiver positioned at the focus point of the dish. The radiation is absorbed through a metallic receiver and generated heat is transferred to a HTF [1,2]. Through the circulation of HTF, heat is collected in a thermal storage system. A dual-axis tracking system is required for the proper collection of heat through the receiver. In the present case, instead of a separate storage system, a cylindrical storage receiver system is used for heat collection and storage. A dish concentrator can be characterized based on its optical and thermal performance. The optical performance is governed by the design parameters of the dish, and the properties of the reflector, while the thermal performance is influenced by the optical performance together with the receiver shape, and the properties of the receiver and HTF materials.

2.1.1. Optical Performance

The concentrator diameter (D), rim angle (ϕ), height (h) and focal distance (f) and local mirror radius (r) are the main responsible design parameters for optical performance (Figure 1). The relations between these parameters are following:

$$f = \frac{D^2}{16h} \tag{1}$$

$$\phi = \sin^{-1}\left(\frac{D}{2r}\right) \tag{2}$$

$$f = \frac{r(1+\cos\phi)}{2} \tag{3}$$

$$r = \frac{1}{2}\sqrt{D^2 + 4(f-h)^2} \tag{4}$$

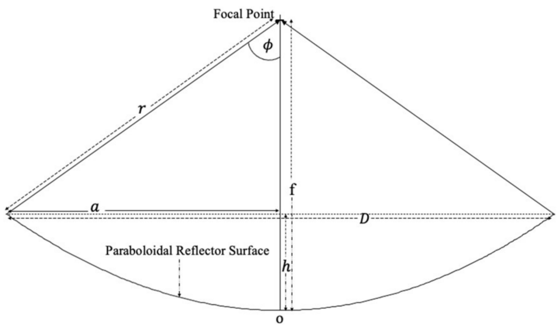

Figure 1. Design parameters of a solar paraboloidal dish concentrator.

The recommended rim angle for a SPDC is between 45 and 67° [1,26]. The numbers of flat reflector facets, the surface errors and the reflectivity of the material are the other influencing parameters of optical design. A finite spread of the focal point can also degrade the optical performance. For an ideal 2D parabola concentrator, the focal image width (F_w) is given as [1]:

$$F_w = \frac{2a\ \sin(\delta)}{\sin\phi\cos(\phi+\delta)} \tag{5}$$

where δ (0.267°) is the sun shape error. The design inadequacy of a dish causes a considerably large practical image width, F_{pw}. So, practically, the ratio of the dish aperture area, A_a, to the receiver base area, A_r, is defined as a characteristic optical performance parameter named as concentration ratio, C_c.

$$C_c = \frac{A_a}{A_r} = \frac{D^2}{F_{pw}^2} \tag{6}$$

2.1.2. Thermal Performance

The high thermal performance of a concentrator is linked with a high optical performance and, the properties of the receiver and HTFs. The optical characteristics of the system affect the rate of available heat (q_a) for thermal application. The rates of utilizable heat (q_u) and the heat loss (q_l) are controlled by the storage receiver system design, and the properties of the receiver and HTF materials. The energy balance equation and the instant thermal efficiency (η_{ith}) for the dish are given as [3]:

$$q_u = q_a - q_l \tag{7}$$

$$q_a = A_a I_b \rho(\gamma\tau\alpha) K_{\gamma\tau\alpha} \tag{8}$$

$$q_l = A_{rs} U_L (T_r - T_a) \tag{9}$$

$$q_u = \left(m_r C_r + m_f C_f\right) \frac{\Delta T_f}{\Delta t} \tag{10}$$

$$\eta_{ith} = \frac{q_u}{q_a} \tag{11}$$

In the above relations, if solar insolation is measured on a horizontal surface, then $I_b = 0.7 I_s \sec\theta$ is a good approximation for the location at Jaipur, where I_b is the beam insolation at the dish aperture area (W/m^2), I_s is the global solar insolation at the horizontal surface (W/m^2), 0.7 is a direct radiation fraction and θ is the angle of incidence on the horizontal surface. Further, ρ is the specular reflectance of the concentrator, τ is the transmittance of receiver cover (if any), γ is the reflected radiation fraction at the receiver surface and α is the absorption coefficient of the absorber. The incidence angle modifier, $K_{\gamma\tau\alpha}$, includes the effects of angle of incidence on the intercept factor. If the receiver has no transparent cover, then the effect of τ and $K_{\gamma\tau\alpha}$ is not considered. The overall heat loss coefficient is U_L. The receiver and ambient temperatures are T_r and T_a, respectively. ΔT_f is the rise in fluid temperature in the time interval Δt, A_{rs} is the receiver total surface area, m_r and m_f are masses of the receiver and fluid, respectively, and, C_r and C_f are specific heats of the receiver and fluid at the constant pressure.

2.2. Characteristic Parameters of Heat Transfer Fluid

The study of a HTF using a concentrator can be performed by conducting the heating and cooling tests in the storage receiver system (SRS).

2.2.1. Heating Test

The heating rate, R_h, and instant thermal efficiency, η_{ith}, are the heating characteristics of a HTF under the transient state. Both can be determined using the linear curve fitting between the fluid temperature, T_f, and heating time i.e., through the thermal profile of the HTF in the concentrator SRS. In the steady state, the HTF reaches to its the maximum fluid temperature, T_{fm}, and remains constant. In a concentrator, T_{fm}, can be normalized through a solar insolation value about 700 W/m^2, to compare T_{fm} of different HTFs tested under variable insolation conditions. Therefore, in the steady state, a new parameter, normalized maximum fluid temperature, T_{nf}, can be introduced. Hence, following are the characteristics of heating test:

In the transient state

$$R_h = \frac{\Delta T_f}{\Delta t} \tag{12}$$

In the steady state

$$R_h = 0$$

$$T_{nf} = \frac{700\overline{\boldsymbol{T_{fm}}}}{\overline{\boldsymbol{I_b}}} \tag{13}$$

where $\overline{\boldsymbol{T_{fm}}}$ and $\overline{\boldsymbol{I_b}}$ are the average maximum fluid temperature and the average beam radiation, respectively, during the steady state.

2.2.2. Cooling Test

The overall heat loss coefficient, U_L, of the SRS can be determined using the HTF cooling curve in absence of sun light. For this, Equation (9), the rate of heat loss $\boldsymbol{q_l'}$ can be re-written in the cooling mode by considering T_r equal to T_f. Accounting newton's law of cooling, the U_L can be determined as follow:

$$\boldsymbol{q_l'} = \boldsymbol{A_{rs} U_L (T_f - T_a)} \tag{14}$$

$$q_l' = (m_r C_r - m_f C_f) R_c \tag{15}$$

$$R_c = \frac{dT_f}{dt} \tag{16}$$

$$\frac{1}{\tau_c} = \frac{\Delta R_c}{\Delta(T_f - T_a)} \tag{17}$$

$$U_L = \frac{(m_r C_r - m_f C_f)}{\tau_c A_{rs}} \tag{18}$$

2.3. Storage Receiver System

For an SPDC, receivers' types are (i) external and (ii) cavity. In the external receiver, the solar flux is absorbed through the exterior material, while in the cavity, the flux is absorbed by the material located inside the cavity. Various shapes of receivers for example cylindrical, spherical, conical, etc., have been studied for concentrators. The simplest design is the external cylindrical receiver that collects the heat and also stores heat for other useful applications. The conventional receiver materials are copper, aluminum and stainless steel (Table 2). High thermal conductivity (417 W/mK) and temperature stability (1084 °C), and moderate density (8940 kg/m^3) are some appropriate properties of copper for use in high temperature concentrator receivers. However, its high cost (INR 500/kg) limits its use in low and medium temperature concentrators. High temperature stability (1510 °C); moderate density (7500 kg/m^3) and low price (INR 190/kg) are good features of a stainless-steel receiver, but the poor thermal conductivity (14.4 W/mK) limits its applications in solar collectors. Good thermal conductivity (237 W/mK) and stability (660 °C) and low density (2712 kg/m^3) and low price (INR 200/kg) make aluminum the most applicable receiver material for the use in low to medium temperature concentrators.

3. Designing of the Solar Dish Concentrator

A small solar paraboloidal dish concentrator was locally fabricated at the Solar Energy Research Laboratory (SERL), University of Rajasthan, Jaipur [3,24]. The design parameters of the dish are taken as per Equations (1)–(5). The diameter of the dish is 1.21 m. For design ease, the paraboloidal curvature is kept shallow by maintaining a large rim angle of 67°. Accordingly, the height and the focal length of the dish are 0.20 m and 0.45 m, respectively. The focal image width for these parameters is 0.016 m for an ideal condition as per Equation (4). However, in a practical scenario, a finite spread of 0.12 m at the focus is observed. The dish consists of a paraboloidal base structure of Galvanized Iron (GI) sheets, a mounting pipe, a receiver stand, a jack system, two sensor-based gear systems and four base wheels. The details of the components are shown in Figure 2. The complete system is light in weight and easy to transport through the four base wheels.

3.1. Paraboloidal Structure

About 17 trapezoid lightweight polymer acrylic reflector sheets are pasted and fixed on the GI sheets. The height of a trapezoid sheet is 0.58 m, and the top and bottom parallel side lengths are 0.225 m and 0.025 m, respectively. Good reflectivity (80%), high flexibility, good temperature stability, and light weight are the important features of an acrylic reflector. The Galvanized Iron structure is bolted on a vertical pole having an elevation tracking arrangement.

3.2. Tracking

For the azimuthal (east to west) tracking, a solar tracker is mounted horizontally between a couple of vertical poles with a central movable axis, Figure 3a. When this horizontal stepper motor (gear mechanism) rotates, the entire dish shifts proportionately about its central pivot, either towards the east or west to track the sun. A set of light-dependent resistors (LDRs) are positioned on a horizontal stand connected to a central movable axis, Figure 3b. This horizontal stand is sufficiently apart from the main structure to provide clear solar radiation signals to LDRs. The LDR signals are received, compared and interpreted by an electronic circuit (consisting of a single IC 324 and two Op-amps) that commands the motor for the azimuthal tracking of the sun. The circuit configuration is shown in Figure 3d. For the altitude/elevation tracking, a jack mechanism is provided just below the paraboloidal structure shown in Figure 3c. The elevation angle is adjusted manually through the motion of a horizontal shaft attached to the jack system.

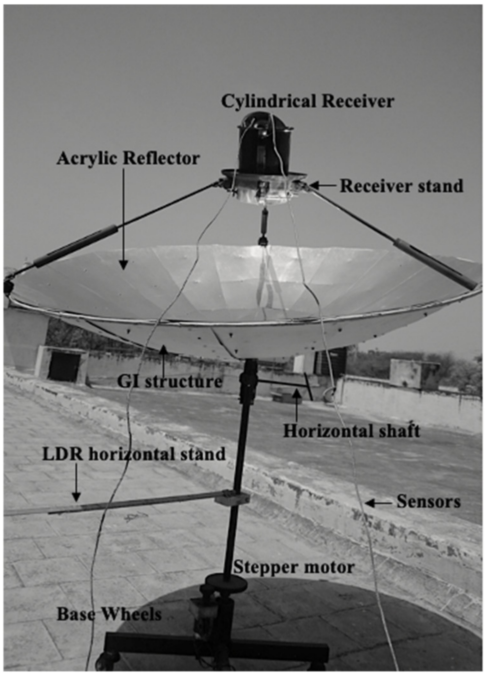

Figure 2. Details of dish components.

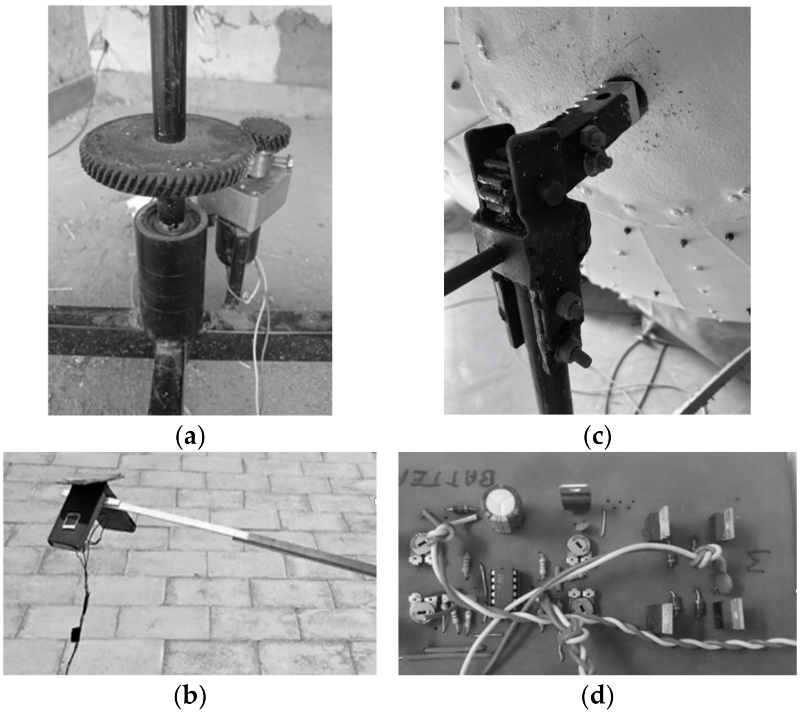

Figure 3. (**a**): Azimuthal tracking. (**b**): LDR arrangement. (**c**): Elevation tracking. (**d**): Tracking circuit.

3.3. Receiver

For this comparative study of HTFs, a simple cylindrical aluminum exterior receiver is used based on the suitable properties of aluminum for medium temperature applications described in Section 2.3. The receiver diameter and height are 0.12 m and 0.175 m, respectively. The weight and maximum fluid capacity are 0.2 kg and 1.2 L, respectively. The base area, A_r, is 0.011 m^2, so the concentration ratio, C_C, is about 100. The receiver is two layers quoted with black matt paint with an absorptivity of 0.90. The receiver is closed with a lid having two holes to insert sensors. The total surface area, A_{rs}, of this cylindrical receiver is 0.088 m^2. The receiver is mounted on a circular receiver stand which is attached to the Galvanized Iron structure using the 3 metallic rods. The lengths of roads are adjustable, and they provide the facility to locate the receiver at the desired position.

4. Selection of HTFs

The selection of an appropriate HTF for solar dish concentrator is based on various physical and chemical properties of a fluid which include: (i) a boiling temperature higher than 150 °C for use in medium temperature applications, (ii) good thermal conductivity for fast heat collection and rejection, (iii) good specific heat for heat storage purposes, (iv) low viscosity for easy fluid motion, (v) low density for a lighter HTF unit, (vi) not toxic or environmentally hazardous and (vii) economically viable. The current state-of-art in introduction reports that various sensible heat transfer fluids have been tested and studied but studies of silicon oil (SO) and ethylene glycol (EG) are limited for concentrator applications, whereas engine oil (EO) has been barely studied. Therefore, based on the local availability and appropriate HTF properties, three HTFs, silicone oil (SO), engine oil (EO) and ethylene glycol (EG) are used for the present study. The properties of these HTFs are listed along with water (a low-temperature HTF) and Therminol 66 (a high-temperature HTF) in Table 3. The suitability of these fluids is supported by various properties mentioned in the table. Therminol 66 is mostly the preferred HTF, but the high cost of this fluid limits its usage in medium temperature applications not economically viable. Table 3 presents a comparison of selected fluids and their properties with Therminol 66. This comparative study favors the suitability of SO, EO and EG for medium temperature applications. All these HTFs have a boiling temperature higher than 170 °C. The thermal conductivities, specific heats and densities are within an acceptable range. The significantly high viscosity of SO, and toxicity of EO and EG are some constraints for their usage. Nevertheless, the present experimental study is conducted to investigate their thermal properties. Water is a low temperature HTF; however, in this comparative experimental study, it is also considered. The ethylene glycol (HELISOL®) is 99% pure, purchased from Merck Life Science Pvt. Ltd. The silicon oil (350 CST) is purchased from Ases Chemicals works and Diesel engine oil (20W-40) is made by Hindustan petroleum Cor. Ltd., Mumbai, India

Table 3. Properties of heat transfer fluids [5,6,14,27–31].

Properties	Water	Silicone Oil	Engine Oil	Therminol 66	Ethylene Glycol
Density (kg/m^3 at 25 °C)	1000	900	870	1008	1113
Flash point (°C)	-	315	238	184	126
Auto ignition Temperature (°C)	-	450	>234	374	427
Boiling point (°C)	100	>250	>176	359	197
Critical temperature (°C)	374	-	434	569	446
Kinematic Viscosity, cSt (100 °C)	0.2938	10–1000	12.5–16	3.77	1.99
Thermal Conductivity (20 °C) (mW/K)	0.6	0.10	0.13	0.12	0.25
Specific Heat (50 °C) (kJ/kg°C)	4.186	1.7	2.1	2.1	2.4
Toxicity	No	Low	Highly	Low	Highly
Environmental Hazards	Friendly	Moderate	High	Moderate	High
Approximate cost INR (per liter)	30	800	200	3000	400

5. Experimental Study

5.1. Test Set-Up

The sensible heating tests for all the HTFs were conducted at the SERL, Jaipur (26.92° N, 75.87° E). The experiments were carried out for a period around local noon, i.e.,11:00 am to 01:00 pm Indian Standard Time (IST) in the month of November 2021. The amount of each HTF was 0.5 L in the cylindrical aluminum receiver. The receiver was covered with a lid and two K-type temperature sensors (range −10 °C to 600 °C) were dipped in the fluid through holes in the lid for fluid temperatures (T_{f1} and T_{f2}) measurement. One sensor was also adjusted at the bottom of the receiver for the base temperature (T_b) measurement. These K-type sensor temperatures were attached to a data logger (Masibus 85XX+, least count 0.1 °C). The data logger is connected to a computer that uses mSCAN+ software to display and record the data in every 5-min interval. The solar insolation (I_s, accuracy ± 5 W/m^2) on the horizontal surface and the ambient temperature (T_a, accuracy ± 0.1 °C) were recorded by a weather station (Virtual hydromet). The manual elevation tracking of the dish concentrator was performed at 15-min intervals and the azimuthal tracking was controlled by an LDR tracking circuit. The cooling test was performed just after the completion of the heating experiment. For this, the dish is moved to a shaded place and the receiver was removed from the receiver stand to avoid conduction losses. The receiver was kept in the shaded open environment of similar ambient temperature conditions of the heating test and the fluid temperatures were measured at 2-min intervals for the 1 h duration.

5.2. Thermal Profiles

The experiments were conducted on a number of days with similar weather conditions of the insolation and ambient temperature within the range of 570 ± 40 W/m^2 and 29 ± 2 °C, respectively, for this comparative study. The measured base temperatures (T_b) and the average fluid temperatures (T_f) on the sunny days are shown in Figure 4. The experimental days for EO, EG, SO and water were 15 November, 17 November, 20 November and 23 November 2021, respectively. These nearby days provided similar weather conditions for comparison. The variation of solar insolation (I_s) and the ambient temperature (T_a) at Indian standard time (IST) on different experimental days are depicted in Figure 5. The fluid capacity is 0.5 L in each experiment. In the transient states, the heating curves of the HTFs are shown in Figure 6. The cooling curves of HTFs are plotted in Figure 7. To examine the effect of high solar insolation, a test with 0.5 L SO is also conducted on a high insolation day. The thermal profile of this test is plotted in Figure 8.

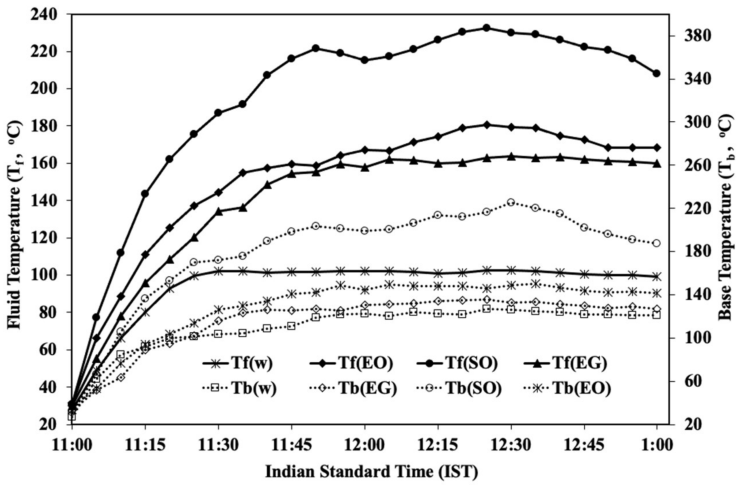

Figure 4. Thermal profiles of different heat transfer fluids (EO 15 November, EG 17 November, SO 20 November, and Water 23 November 2021) of capacity 0.5 L each in dish concentrator receiver (T_b and T_f are receiver base and average fluid temperature, respectively).

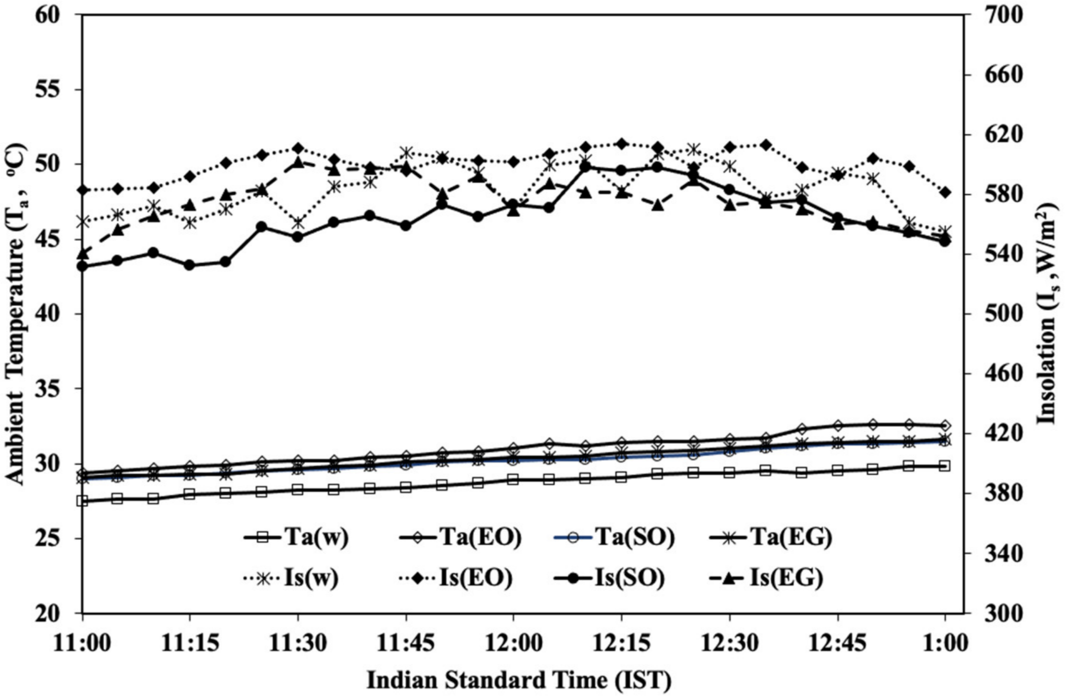

Figure 5. Variation of solar insolation (I_s) and ambient temperature (T_a) with Indian standard time (IST) on experimental days, EO 15 November, EG 17 November, SO 20 November and Water 23 November 2021.

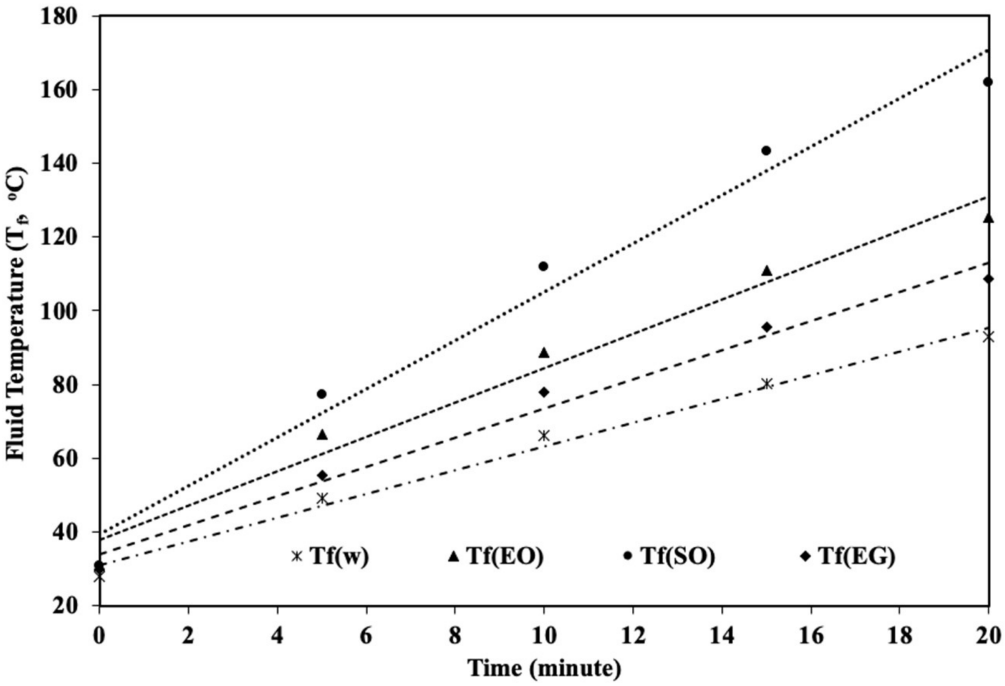

Figure 6. Heating curves of HTFs in transient state (EO 15 November, EG 17 November, SO 20 November and water 23 November 2021).

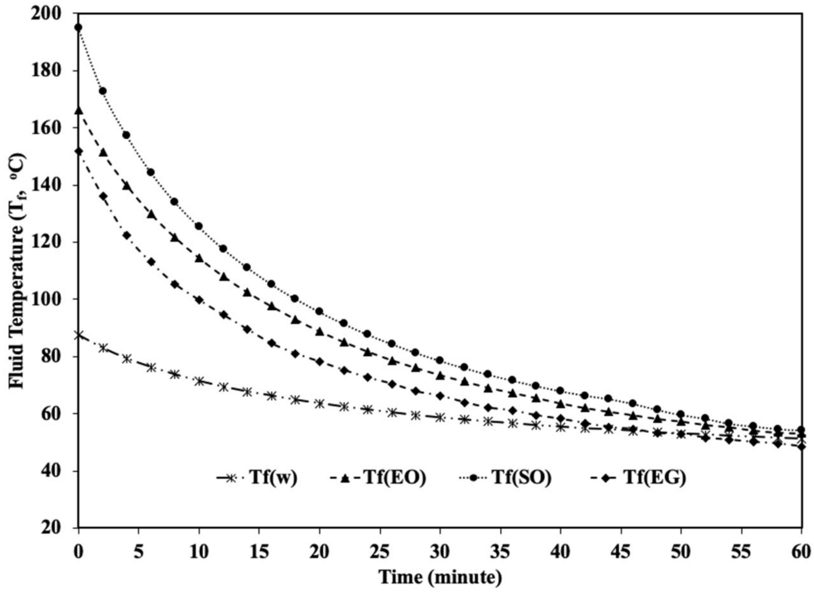

Figure 7. Cooling curves of HTFs (EO 15 November, EG 17 November, SO 20 November and water 23 November 2021).

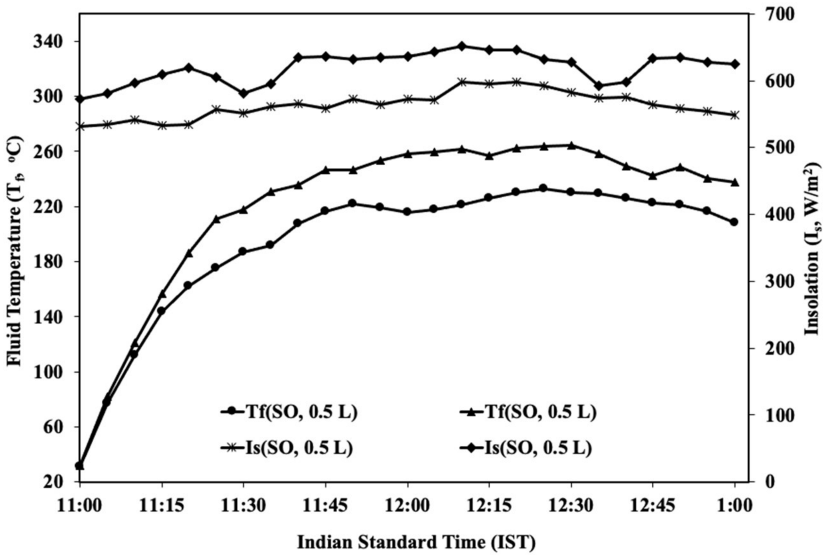

Figure 8. Variation of solar insulations (I_S) and average fluid temperatures (T_f) with Indian standard time (IST) for SO of capacity 0.5 L (20 November 2021) and 0.5 L (09 November 2021).

6. Result and Discussion

6.1. Thermal Performance of the Developed Concentrator

Figure 4 illustrates that in the transient state, the temperatures of fluids increase at a good rate (3.21 to 6.56 °C/s) and temperatures reach a steady state (100 to 230 °C). As the solar insolation decreases in the afternoon hours, the fluid temperature slightly decreases. The transient state time varies for different fluids, but an effective transient time of 20 min can be considered to determine the rate of heating. The highest fluid temperature is about 230 °C, corresponding to the solar insolation of 550 W/m^2. The thermal efficiency for water load is found to be 41%, which is near to the efficiency values quoted in Table 2 references [20,21]. It reflects the good thermal performance of the concentrator for low to medium-temperature solar thermal applications via a suitable heat transfer fluid. No sudden decrease or increase is observed in the thermal profiles, indicating the appropriate working of the LDR-based tracking system on sunny days.

6.2. Characteristics of HTFs

The base and fluid temperatures of the storage receiver system are depicted in Figure 4 for the selected fluids. The solar insolation and ambient temperature variations on these experimental days are shown in Figure 5. The solar insolation and the ambient temperature variations are in the range of about 570 ± 40 W/m^2 and 29 ± 2 °C, respectively, on the test days. These considerably small variations provide an identical condition to compare the performance of selected HTFs. Figure 4 clearly depicts that the silicone oil temperature reaches near 230 °C which is much higher than any other fluid. The highest temperatures for other HTFs, engine oil, ethylene glycol and water, are 180 °C, 160 °C and 100 °C, respectively. The ambient temperatures remained close to each other for all the experimental days. From Figure 5, the insolation values corresponding to the highest temperatures of all fluids are within a variation of about 595 ± 10 W/m^2. The heating curves in the transient time period of 20 min are plotted in Figure 6. In the initial 20 min, the temperatures attained by SO, EO, EG and water are 162, 125, 109 and 93 °C, respectively. This figure depicts that the highest rate of fluid temperature rise occurred for silicone oil. The cooling curves of all fluids are depicted in Figure 7. In the cooling tests, the temperatures of SO, EO, EG and water decreased at different rates and reached near 50 °C after one hour. The heating and cooling characteristic parameters are determined using Figures 4–7 and Equations (7)–(18), and are given in Tables 4 and 5. For this computation, γ is taken as 0.8 and the average value of θ is considered to be 48° for noon time in the month of November. The properties of fluids are taken from Table 3 for the computation of the rates of utilizable heat. Table 4 infers that the rates of the available heat differ within 395 ± 25 W which offers similar weather conditions to compare the characteristic parameters. Using the values of the rates of heat available and utilizable, the instant efficiency of each fluid is computed. The instant efficiency is found to be 43% for silicone oil (SO), while EO, EG and water have efficiencies of 36%, 31% and 41%, respectively. Water has good efficiency for low temperature applications. Table 5 contains the heating and cooling characteristics of HTFs. In this table, R_g represents the regression coefficient of the heating curve in the transient state and the linear curve between R_c and $T_f - T_a$ in the cooling test. The ambient temperature for the cooling test is considered to be the same for one hour. The ambient temperature values were near 31.5, 32.5, 31.6 and 29.8 °C during the cooling tests of SO, EO, EG and water, respectively. All the linear curves have R_g greater than 0.90, showing good approximations for linear relationships. The heating rate of a HTF (R_h), 6.56 °C/s, is found to be maximum for SO (due to low specific heat) and minimum 3.21 °C/s for water (due to the highest specific heat). The normalized maximum fluid temperature, T_{nf}, is determined to be 274 °C for SO from the thermal profile on 20 November. From Figure 8, the average fluid temperature attained by SO is 254 °C at the average insolation of 630 W/m^2 on 9 November 2021 and the T_{nf} is found to be 282 °C. These values of, T_{nf}, on 20 November and 9 November are within the range of 278 ± 4 °C, so the normalized maximum fluid temperature can be a characteristic of any HTF. The overall heat loss coefficient, U_L, during cooling is found 14 W/mK for SO, which is the lowest compared to the other fluids. This is due to the increase in the specific heat of SO from 1.7 kJ/kg°C (at 50 °C) to 2.1 kJ/kg°C (at 250 °C).

Table 4. Instant thermal efficiency of HTFs.

Time (min)	Heat Transfer Materials											
	q_a (W)				q_u(W)				η_{ith} (%)			
	W	EG	EO	SO	W	EG	EO	SO	W	EG	EO	SO
0	389	374	403	368	160	103	145	159	41	31	36	43
5	392	385	404	370	130	82	91	120	33	27	23	32
10	396	398	405	374	105	59	91	108	27	21	23	29
15	388	403	410	369	95	53	59	64	25	15	14	17
20	395	401	416	370	51	64	49	47	13	13	12	13
25	403	404	420	386	20	10	29	39	5	6	7	10

Table 5. HTF heating and cooling characteristics.

HTF	Heating Curve						Cooling Curve		
	Transient State				Steady State		R_c vs. $(T_f - T_a)$ Curve		
	R_g	R_h (°C/s)	Max. η_{ith} (%)	$\overline{T_{fm}}$(°C)	$\overline{I_s}$ (W/m^2)	T_{nf} (°C)	R_g	τ_c(min)	U_L(W/mK)
Water	0.99	3.21	41	101	588	120	0.96	17	26
EG	0.98	3.95	31	161	571	198	0.96	11	23
EO	0.98	4.66	36	173	603	200	0.98	15	15
SO	0.98	6.56	45	223	576	274	0.97	14	14

Hence, the transient η_{ith}, R_h, and the steady state heating characteristics, T_{nf}, are found to be highest, and the cooling characteristics U_L is found to be lowest for silicone oil. The physical appearance of all the fluids before heating and after heating was checked. No significant color changes or viscosity changes were observed for SO and EG, but for EO, slight changes were observed. The costs of EO and EG are lower than the SO, but it is observed during experiments that EO and EG have strong fume issues while no such problem is noticed for SO. Overall, based on characteristics parameters and physical and chemical properties, SO is found to be the most suitable HTF for medium temperature solar concentrators for heat transfer and storage applications.

7. Conclusions

The selection of an appropriate heat transfer fluid (HTF) for a solar concentrator enhances its efficiency. This selection depends on the temperature range and physical and chemical stability, together with the economic feasibility of the HTF. Presently, a paraboloidal solar dish concentrator is designed and developed with some attractive features and the thermal performance is tested using four selected HTFs, which are: Silicone oil (SO), Engine Oil (EO), Ethylene Glycol (EG) and Water (W). The characteristic parameters of the thermal efficiency, rate of heating and rate of heat loss coefficient are theoretically explained in the paper and experimentally determined for each HTF. A new characteristic parameter "normalized maximum fluid temperature", provides a way to investigate the generated temperature in similar solar insolation conditions. It is found that the Silicone oil (SO) has a maximum heating rate 6.56 °C/s and a normalized maximum fluid temperature of 274 °C. The overall heat loss coefficient is determined to be a minimum of 14 W/mK for SO. Therefore, the present work suggests Silicone oil as the most suitable HTF for medium temperature heat transfer and storage applications.

Author Contributions: S.K.: Experimental investigation, theoretical data collection, resources and drafting. P.K.K.: Investigation and data collection. M.S.K.: Investigation, data collection and resources. H.P.: Resources, review and editing. A.M.: Technical amendment, formal analysis, visualization, expert language suggestions, review and editing. S.M.: Methodology, technical analysis, conceptualization, writing original draft and supervision. All authors have read and agreed to the published version of the manuscript.

Funding: Department of Science and Technology (Project No. DST/TMD/SERI/S91), Science and Engineering Research Board (Project No. EEQ/2018/000811).

Acknowledgments: This research is carried out at the solar energy research laboratory (SERL), Department of Physics, University of Rajasthan, Jaipur as a part of two project works, and these projects (DST/TMD/SERI/S91 and EEQ/2018/000811) are funded by the Department of Science and Technology (DST) and Science and Engineering Research Board (SERB), New Delhi, India. Pawan Kuldeep and Sandeep Kumar are thankful to UGC, New Delhi, India for providing fellowships to them to carry out this research work.

Conflicts of Interest: The authors declare that they have no known competing financial interests or personal relationships that could have appeared to influence the work reported in this paper. All of the sources of funding for the work described in this publication are acknowledged. It is confirmed that the manuscript has been read and approved by all named authors and the order of authors listed in the manuscript has been approved by all named authors.

Nomenclature

α	absorption coefficient of the absorber
γ	reflected radiation fraction at the receiver surface
δ	sun shape error (°)
η_{ith}	instant thermal efficiency
θ	angle of incidence on the horizontal surface (°)
ρ	specular reflectance of the concentrator
τ	transmittance of receiver cover material
τ_c	cooling time characteristic (s)
ϕ	rim angle (°)
A_a	dish aperture area (m^2)
A_r	receiver base area (m^2)
A_{rs}	receiver total surface area (m^2)
C_c	concentration ratio
C_f	specific heat of fluid at the constant pressure (J/kg°C)
C_r	specific heat of receiver (J/kg°C)
D	concentrator diameter (m)
F_w	focal image width (m)
F_{pw}	practical focal image width (m).
f	focal distance (m)
h	height (m)
I_b	beam radiation at dish aperture area (W/m^2),
I_s	global solar insolation on horizontal surface (W/m^2),
$K_{\gamma\tau\alpha}$	incidence angle modifier
m_r	receiver mass (kg)
m_f	fluid mass (kg)
q_a	rate of available heat (W).
q_u	rate of utilizable heat (W)
q_l	rate of heat loss (W)
r	local mirror radius (m)
R_h	heating rate of HTF (°C/s)
R_c	cooling rate of HTF (°C/s)
T_f	fluid temperature (°C)
T_{fm}	maximum fluid temperature (°C)
T_{nf}	normalized maximum fluid temperature (°C)
T_r	receiver temperature (°C)
T_a	ambient temperature (°C)
ΔT_f	rise in fluid temperature in the Δt time interval (°C)
U_L	overall heat loss coefficient (W/mK),
CSP	concentrated solar power
EG	ethylene glycol
EO	engine oil
HTF	heat transfer fluid
LDR	light-dependent resistor
SO	silicone oil
SPDC	solar paraboloidal dish concentrator
STC	solar thermal collector
STS	solar thermal systems
SRS	storage receiver system
TES	thermal energy storage

References

1. Duffie, J.A.; Beckman, W.A. *Solar Energy Thermal Processes*; New York John Willy and Sons: Hoboken, NJ, USA, 1974.
2. Boerema, N.; Morrison, G.; Taylor, R.; Rosengarten, G. Liquid sodium versus Hitec as a heat transfer fluid in solar thermal central receiver systems. *Sol. Energy* **2012**, *86*, 2293–2305. [CrossRef]
3. Mahavar, S.; Bhardwaj, A.; Dashora, P. Fabrication and testing of a light weight solar concentrator. *Int. J. Solid State Mater.* **2016**, *2*, 1–9.
4. Mahavar, S.; Khan, M.S.; Yadav, T. Synthesis, Characterization and Testing of Black Metal Oxide Nanoparticles as Solar Concentrator Receiver Material. *Mater. Today Proc.* **2019**, *8*, 22–27. [CrossRef]
5. Benoit, H.; Spreafico, L.; Gauthier, D.F. Review of heat transfer fluids in tube receivers used in concentrating solar thermal systems: Properties and heat transfer coefficients. *Renew. Sustain. Energy Rev.* **2016**, *55*, 298–315. [CrossRef]
6. Vignarooban, K.; Xu, X.; Arvay, A.; Hsu, K.; Kannan, A.M. Heat transfer fluids for concentrating solar power systems-A review. *Appl. Energy* **2015**, *146*, 383–396. [CrossRef]
7. Malviya, R.; Agrawal, A.; Baredar, P.V. A Comprehensive review of different heat transfer working fluids for solar thermal parabolic trough concentrator. *Mater. Today Proc.* **2021**, *46 Pt 11*, 5490–5500. [CrossRef]
8. Zaharil, H.A.; Hasanuzzaman, M. Modelling and Performance Analysis of Parabolic Trough Solar Concentrator for Different Heat Transfer Fluids under Malaysian Condition. *Renew. Energy* **2020**, *149*, 22–41. [CrossRef]
9. Conroy, T.; Collins, M.N.; Fisher, J.; Grimes, R. Thermohydraulic analysis of single phase heat transfer fluids in CSP solar receivers. *Renew. Energy* **2018**, *129 Pt A*, 150–167. [CrossRef]
10. Trabelsi, S.E.; Qoaider, L.; Guizani, A. Investigation of using molten salt as heat transfer fluid for dry cooled solar parabolic trough power plants under desert conditions. *Energy Convers. Manag.* **2018**, *15*, 253–263. [CrossRef]
11. Kenda, E.S.; Edem, K.; Tsoukpoe, N.; Igor, W.K.O.; Coulibaly, Y.; Xavier, P.; Marie, F.; Armel, W. Jatropha curcas crude oil as heat transfer fluid or thermal energy storage material for concentrating solar power plants. *Energy Sustain. Dev.* **2017**, *40*, 59–67. [CrossRef]
12. Hoffmann, J.F.; Vaitilingom, G.; Henry, J.F.; Chirtoc, M.; Olives, R.; Goetz, V. Temperature dependence of thermophysical and rheological properties of seven vegetable oils in view of their use as heat transfer fluids in concentrated solar plants. *Sol. Energy Mater. Sol. Cells* **2018**, *178*, 129–138. [CrossRef]
13. Nkwetta, D.N.; Smyth, M.; Zacharopoulos, A.; Hyde, T. Experimental performance analysis and optimization of medium temperature solar thermal collectors with silicon oil as a heat transfer fluid. *Int. J. Energy Res.* **2013**, *37*, 570–581. [CrossRef]
14. Jung, C.; Dersch, J.; Nietsch, A.; Senholdt, M. Technological Perspectives of Silicone Heat Transfer Fluids for Concentrated Solar. *Power Energy Procedia* **2015**, *69*, 663–671. [CrossRef]
15. Peng, Q.; Ding, J.; Wei, X.; Yang, J. The Preparation and Properties of Multi-Component Molten Salts. *Appl. Energy* **2010**, *87*, 2812–2817. [CrossRef]
16. Qoaider, L.; Thabit, Q.; Kiwan, S. Innovative Sensible Heat Transfer Medium for a Moving Bed Heat Exchanger in Solar Central Receiver Power Plants. *Appl. Sol. Energy* **2017**, *53*, 161–166. [CrossRef]
17. Perez-Tavernier, J.; Vallejo, J.P.; Cabaleiro, D.; Fernandez-Seara, J.; Lugo, L. Heat transfer performance of a nano-Enhanced propylene glycol:water mixture. *Int. J. Therm. Sci.* **2019**, *139*, 413–423. [CrossRef]
18. Sandhya, J.; Venkatraj, V. Effect of various heat transport fluids on central receiver solar thermal power plant. *Mater. Today Proc.* **2019**, *16 Pt 2*, 314–320.
19. Quederni, A.R.E.; Salah, M.B.; Askri, F.; Nasrallah, M.B.; Aloui, F. Experimental study of a parabolic solar concentrator. *Revue des Energies Renouvelables* **2009**, *12*, 395–404. Available online: https://www.cder.dz/download/Art12-3_6.pdf.
20. Mohammed, I.L. Design and development of a parabolic dish solar water heater. *Int. J. Eng. Res. Appl.* **2012**, *2*, 822–830.
21. Omara, Z.M.; Eltawil, M.A. Hybrid of solar dish concentrator, new boiler and simple solar collector for brackish water desalination. *Desalination* **2013**, *326*, 62–68. [CrossRef]
22. Subramani, J.; Nagarajan, P.K.; Subramaniyan, C.; Anbuselvan, N. Performance studies on solar parabolic dish collector using conical cavity receiver for community heating applications. *Mater. Today Proc.* **2021**, *45 Pt 2*, 1862–1866. [CrossRef]
23. Hassan, A.; Quanfang, C.; Abbas, S.; Lu, W.; Youming, L. An experimental investigation on thermal and optical analysis of cylindrical and conical cavity copper tube receivers design for solar dish concentrator. *Renew. Energy* **2021**, *179*, e1849–e1864. [CrossRef]
24. Mahavar, S.; Goyal, A.; Balakin, B.V. Investigation of a Solar Concentrator for Water Distillation. In *Advances in Thermal Engineering, Manufacturing, and Production Management. ICTEMA 2020. 2021. Lecture Notes in Mechanical Engineering*; Ghosh, S.K., Ghosh, K., Das, S., Dan, P.K., Kundu, A., Eds.; Springer Nature Singapore Pte Ltd.: Singapore. [CrossRef]
25. Kumar, V.; Yadav, A. Experimental investigation of parabolic dish concentrator with various sizes of receiver. *Mater. Today Proc.* **2021**, *44*, 4966–4971. [CrossRef]
26. Reddy, K.S.; Veershetty, G.; Vikram, T.S. Effect of wind speed and direction on convective heat losses from solar parabolic dish modified cavity receiver. *Sol. Energy* **2016**, *131*, 183–198. [CrossRef]
27. Khandelwal, N.; Sharma, M.; Singh, O.; Shukla, A.K. Comparative analysis of the linear Fresnel reflector assisted solar cycle on the basis of heat transfer fluids. *Mater. Today Proc.* **2021**, *38*, 74–79. [CrossRef]
28. Scott, W.; Paul, S.; Harold, P.; Ernest, S.E. Heat Transfer Properties of Engine Oils. In Proceedings of the WTC2005 World Tribology Congress III, Washington, DC, USA, 12–16 September 2005.

29. Yue, H.; Zhao, Y.; Ma, X.; Gong, J. Ethylene glycol: Properties, synthesis, and applications. *Chem. Soc. Rev.* **2012**, *41*, 4218–4244. [CrossRef]
30. Sathish, S.; Kannan, M.; Sathish, B.R.; Johnson, S.S.; Jacob, S. Experimental Analysis of Single Reflector Box Type Solar Cooker with Thermo Fluid. *J. Crit. Rev.* **2020**, *7*, 144–147. [CrossRef]
31. Grirate, H.; Zari, N.; Elmchaouri, A.; Molina, S.; Couturier, R. Life Time Analysis of Thermal Oil Used as Heat Transfer Fluid in CSP Power Plant. *AIP Conf. Proc.* **2016**, *1734*, 040005. [CrossRef]